Supplementary

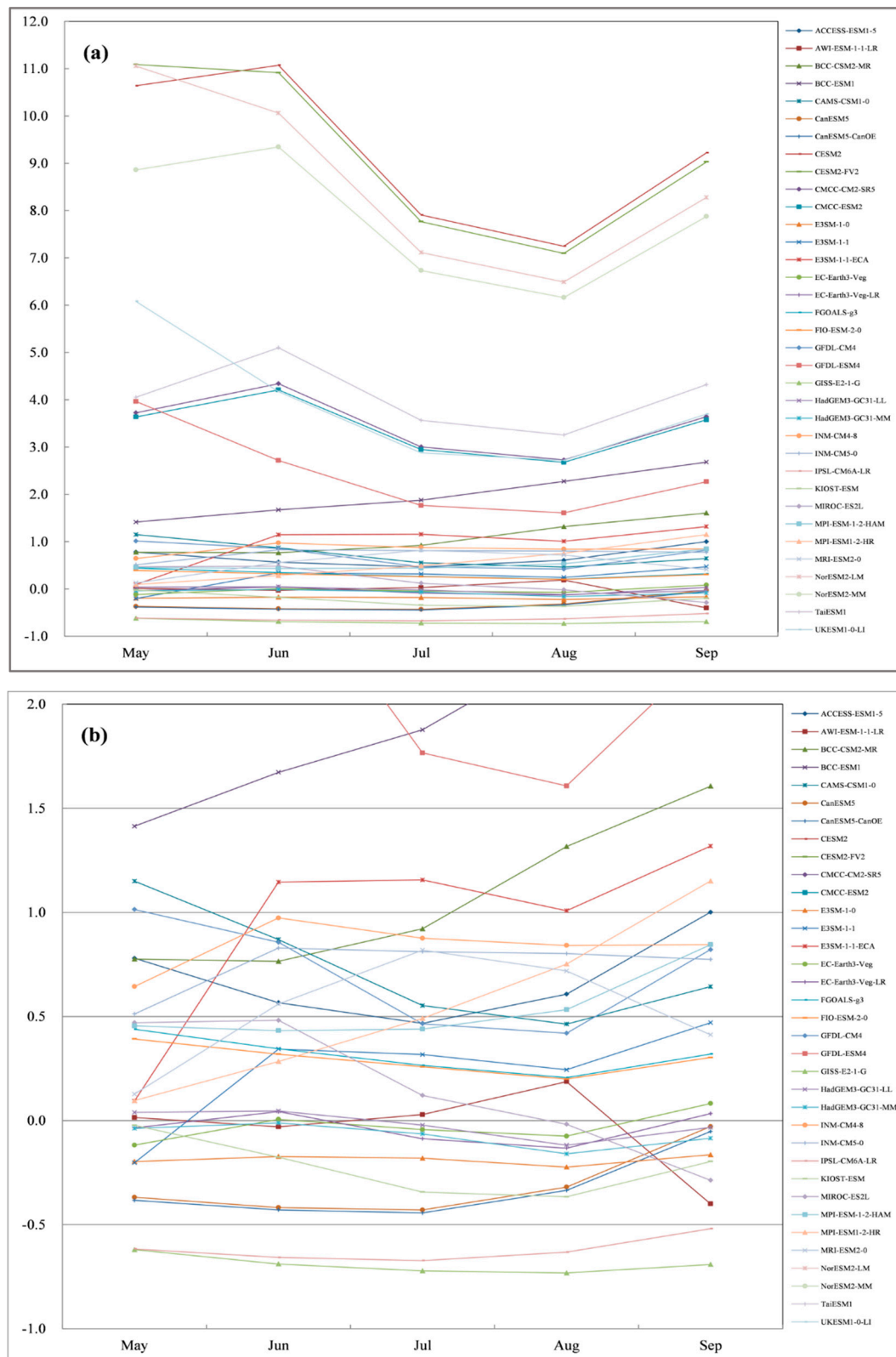**Figure S1**. The relative bias of the monthly LAI of the simulations and observations. The y-axis is from –1 to 12 in (a), and from –1 to 2 in (b).

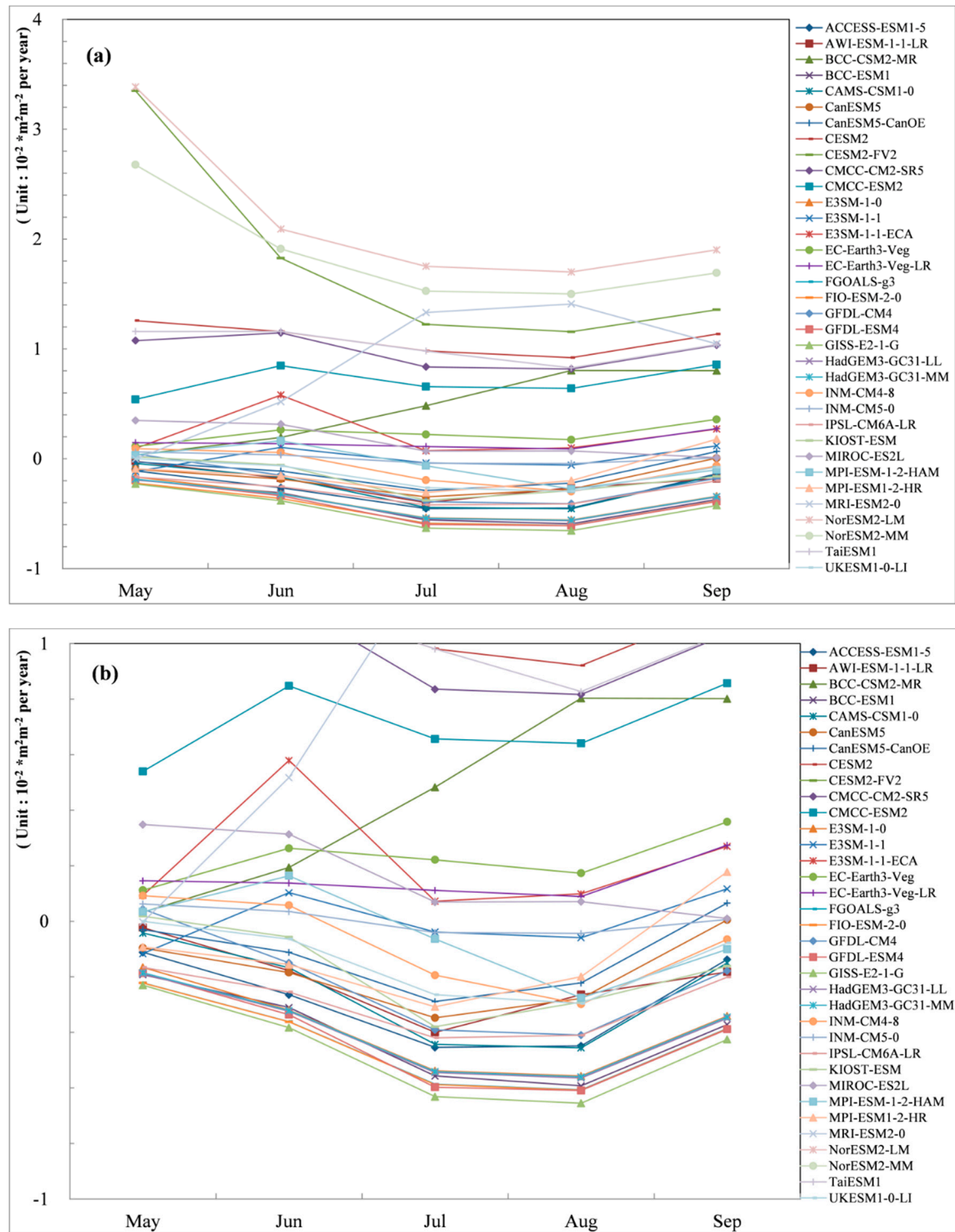**Figure S2**. The bias of the monthly LAI trend with simulations and observations. The y-axis is from –1 to 3.5 in (a), and from –1 to 1 in (b).

Table S1. Summary of evaluation metrics and error ranking for models with the performance to simulate the LAI of Tibetan Plateau during growing season in1981-2014.

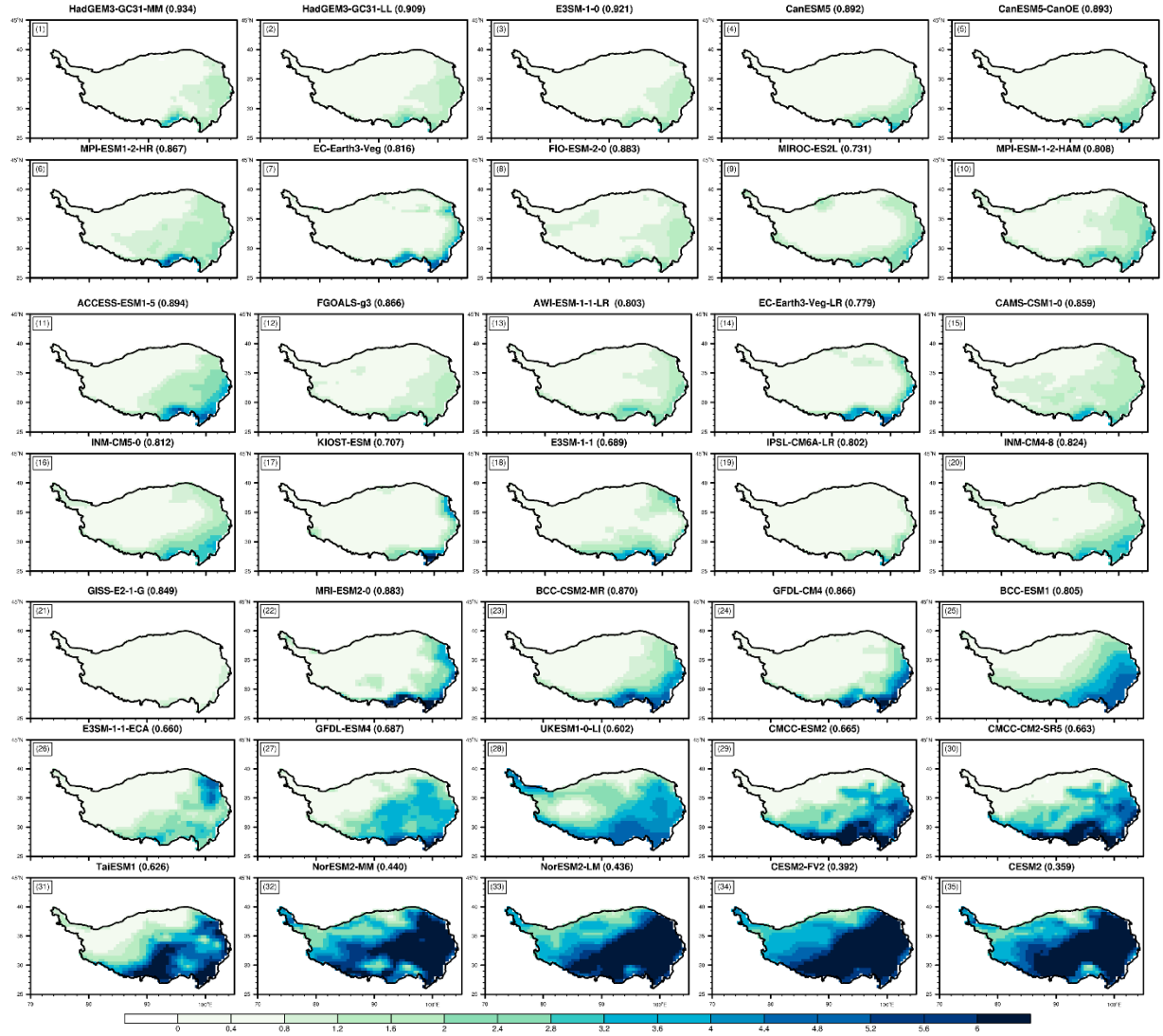| Model	Metrics/Ranking				Error ranking
	Patter_correlation	|Bias|$_{avg}$	RMSE	Ratio	
HadGEM3-GC31-MM	0.934/ 1	0.204/ 1	0.355/ 1	0.696/ 14	1
HadGEM3-GC31-LL	0.909/ 3	0.239/ 3	0.399/ 2	0.658/ 15	2
E3SM-1-0	0.921/ 2	0.216/ 2	0.414/ 3	0.627/ 16	3
CanESM5	0.892/ 6	0.267/ 4	0.416/ 4	0.816/ 10	4
CanESM5-CanOE	0.893/ 5	0.272/ 5	0.421/ 5	0.803 11	5
MPI-ESM1-2-HR	0.867/ 10	0.449/ 16	0.559/ 10	0.919/ 3	6
EC-Earth3-Veg	0.816/ 16	0.394/ 7	0.554/ 9	1.166/ 9	7
FIO-ESM-2-0	0.883/ 8	0.412/ 9	0.519/ 7	0.518/ 18	8
MIROC-ES2L	0.731/ 23	0.420/ 10	0.584/ 11	0.915/ 4	9
MPI-ESM-1-2-HAM	0.808/ 18	0.452/ 17	0.602/ 14	0.945/ 1	10
ACCESS-ESM1-5	0.894/ 4	0.477/ 18	0.678/ 17	0.753/ 12	11
FGOALS-g3	0.866/ 11	0.433/ 13	0.542/ 8	0.499/ 19	12
AWI-ESM-1-1-LR	0.803/ 20	0.380/ 6	0.512/ 6	1.594/ 21	13
EC-Earth3-Veg-LR	0.779/ 22	0.435/ 14	0.594/ 12	1.141/ 8	14
CAMS-CSM1-0	0.859/ 13	0.521/ 19	0.602/ 13	0.733/ 13	15
INM-CM5-0	0.812/ 17	0.572/ 22	0.676/ 16	0.888/ 5	16
KIOST-ESM	0.707/ 24	0.428/ 11	0.684/ 18	1.113/ 7	17
E3SM-1-1	0.689/ 25	0.449/ 15	0.693/ 19	1.069/ 2	18
IPSL-CM6A-LR	0.802/ 21	0.398/ 8	0.629/ 15	0.623/ 17	19
INM-CM4-8	0.824/ 15	0.599/ 23	0.701/ 20	0.887/ 6	20
GISS-E2-1-G	0.849/ 14	0.432/ 12	0.759/ 21	0.281/ 25	21
MRI-ESM2-0	0.883/ 7	0.541/ 20	0.923/ 23	1.808/ 28	22
BCC-CSM2-MR	0.870/ 9	0.689/ 24	0.993/24	1.594/ 22	23
GFDL-CM4	0.866/ 12	0.545/ 21	0.917/ 22	1.733/ 26	24
BCC-ESM1	0.805/ 19	1.254/ 26	1.547/ 26	1.744/ 27	25
E3SM-1-1-ECA	0.660/ 29	0.732/ 25	1.122/ 25	1.512/ 20	26
GFDL-ESM4	0.687/ 26	1.382/ 27	1.722/ 27	1.717/ 24	27
UKESM1-0-LI	0.602/ 31	2.199/ 30	2.440/ 28	1.616/ 23	28
CMCC-ESM2	0.665/ 27	2.038/ 28	2.635/ 29	2.605/ 29	29
CMCC-CM2-SR5	0.663/ 28	2.083/ 29	2.682/ 30	2.628/ 30	30
TaiESM1	0.626/ 30	2.407/ 31	3.020/ 31	2.709/ 31	31
NorESM2-MM	0.440/ 32	4.559/ 32	5.020/ 32	2.839/ 32	32
NorESM2-LM	0.436/ 33	4.954/ 33	5.420/ 33	2.960/ 33	33
CESM2-FV2	0.392/ 34	5.332/ 34	5.803/ 34	3.032/ 34	34
CESM2	0.359/ 35	5.387/ 35	5.977/ 35	3.385/ 35	35

Figure S3. Spatial distributions of the simulated LAI during the growing season. The number in parentheses in Figure S3 show the pattern correlation value between the simulations and observations.
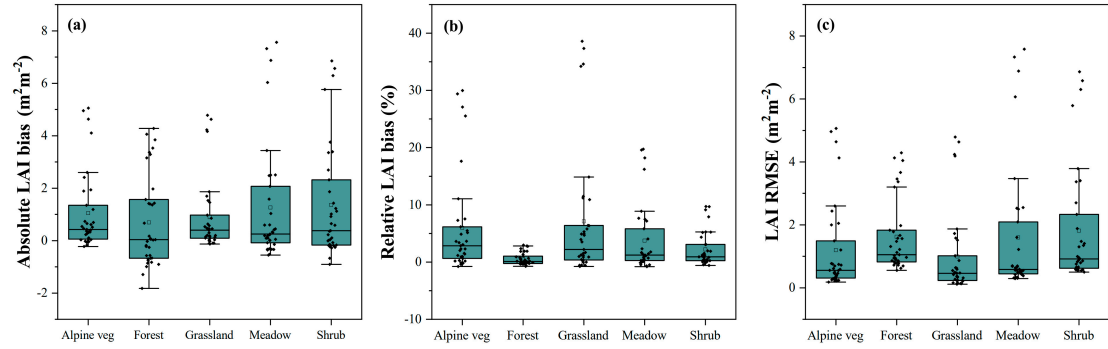
Figure S4. The distribution of bias, relative bias and RMSE between the simulated and observed LAI with 35 CMIP6 models for different vegetation types; the LAI is the averaged LAI during the growing season in1981-2014.
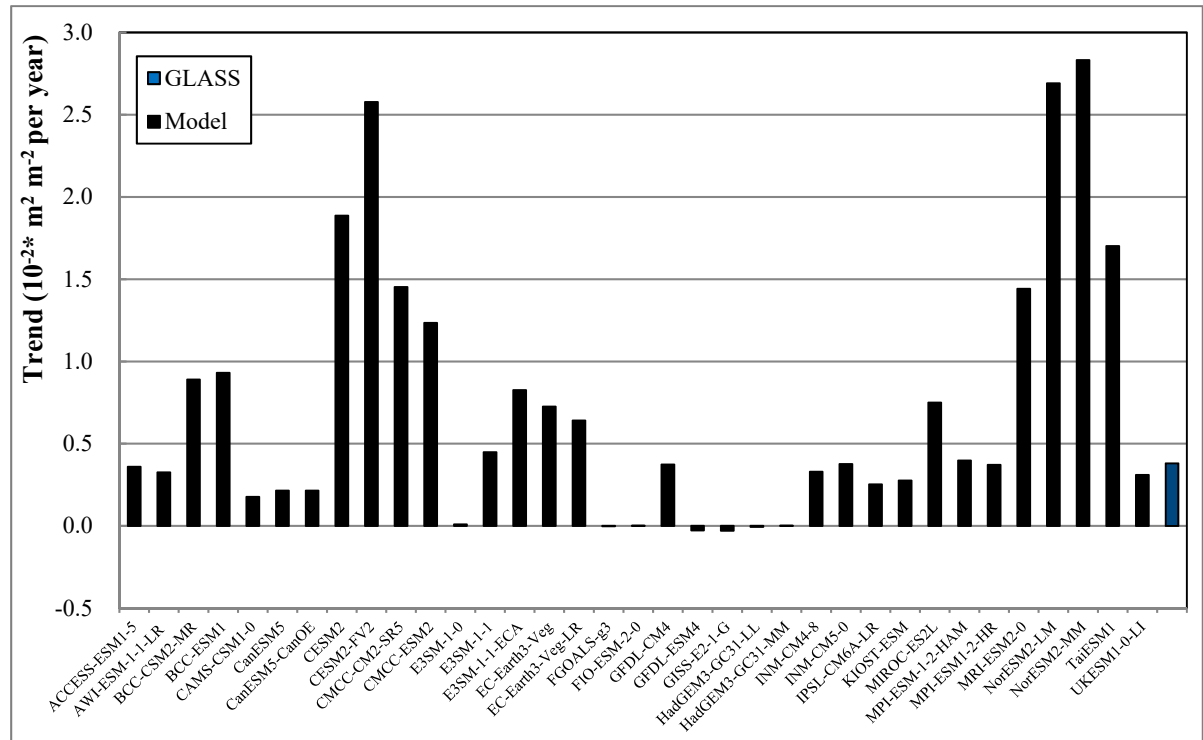

Figure S5. The area-averaged linear trend of simulated and observed LAI the during the growing season (p < 0.05)

Table S2. Summary of evaluation metrics and error ranking for models with the performance to simulate the LAI trend of Tibetan Plateau during growing season in1981-2014.

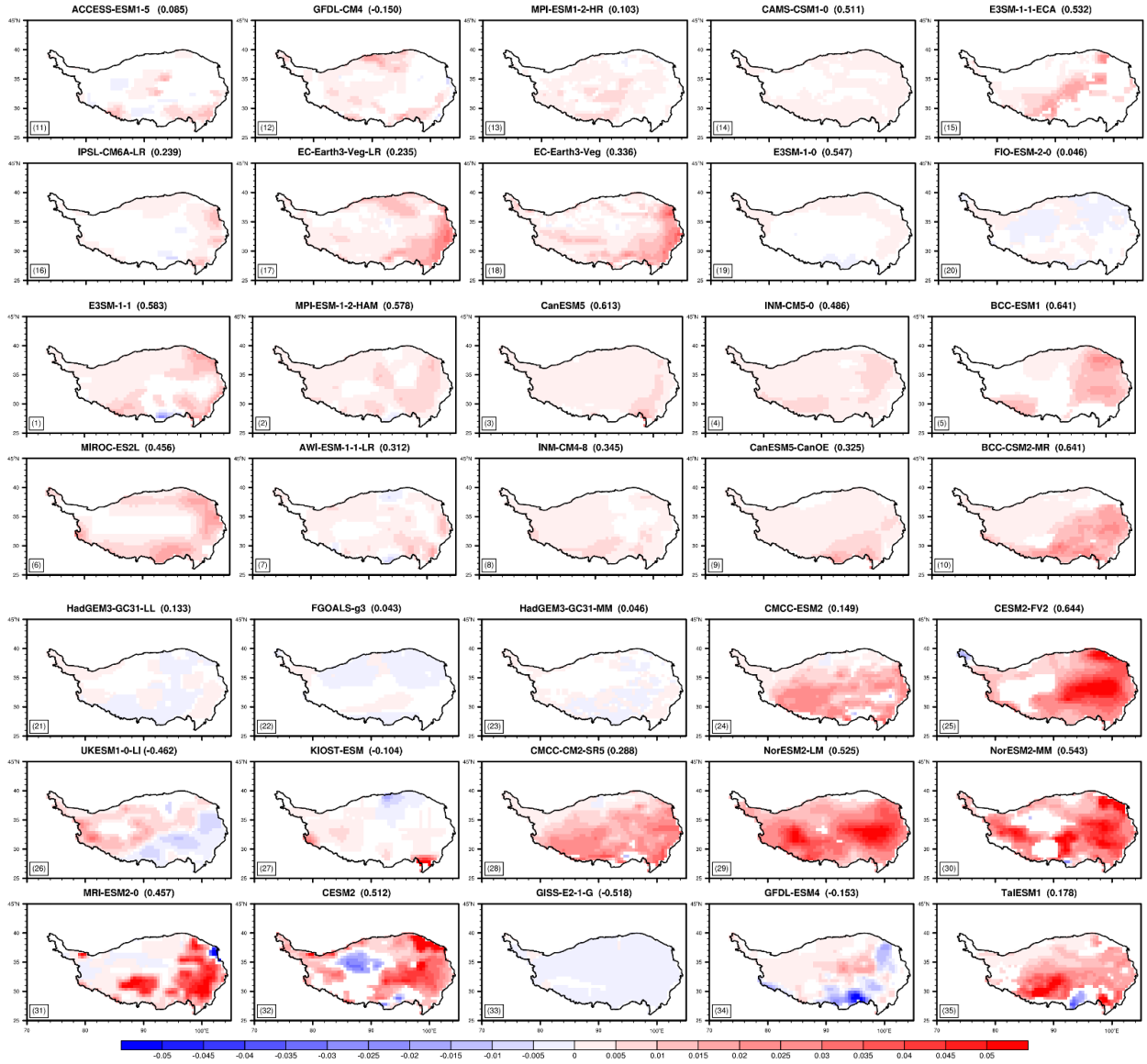| Model	Metrics/Ranking				Error ranking
	Patter_correlation	$Bias_{avg}(10^{-3})$	$RMSE(10^{-3})$	Ratio	
E3SM-1-1	0.583/ 5	2.585/ 1	4.091/ 2	1.112/ 2	1
MPI-ESM-1-2-HAM	0.578/ 6	2.765/ 2	3.979/ 1	0.567/ 10	2
CanESM5	0.613/ 4	3.113/ 6	4.702/ 6	0.524/ 11	3
INM-CM5-0	0.486/ 13	2.969/ 4	4.242/ 3	0.306/ 17	4
BCC-ESM1	0.641/ 3	4.840/ 16	6.060/ 14	1.175/ 5	5
MIROC-ES2L	0.456/ 15	3.994/ 12	5.514/ 11	1.067/ 1	6
AWI-ESM-1-1-LR	0.312/ 19	3.045/ 5	4.710/ 7	0.651/ 9	7
INM-CM4-8	0.345/ 16	2.807/ 3	4.391/ 4	0.294/ 18	8
CanESM5-CanOE	0.325/ 18	3.231/ 8	5.007/ 9	0.733/ 7	9
BCC-CSM2-MR	0.641/ 2	4.672/ 14	6.759/ 16	1.487/ 12	10
ACCESS-ESM1-5	0.085/ 27	3.556/ 10	5.071/ 10	0.883/ 3	11
GFDL-CM4	-0.150/ 32	3.253/ 9	4.746/ 8	0.849/ 4	12
MPI-ESM1-2-HR	0.103/ 26	3.115/ 7	4.456/ 5	0.362/ 16	13
CAMS-CSM1-0	0.511/ 12	3.989/ 11	5.804/ 12	0.186/ 20	14
E3SM-1-1-ECA	0.532/ 9	5.517/ 24	7.089/ 21	1.331/ 8	15
IPSL-CM6A-LR	0.239/ 21	5.069/ 18	7.066/ 20	0.764/ 6	16
EC-Earth3-Veg-LR	0.235/ 22	5.054/ 17	7.064/ 19	1.536/ 13	17
EC-Earth3-Veg	0.336/ 17	5.109/ 20	7.312/ 23	1.604/ 15	18
E3SM-1-0	0.547/ 7	5.305/ 21	7.371/ 24	0.036/ 23	19
FIO-ESM-2-0	0.046/ 28	4.230/ 13	6.024/ 13	0.022/ 25	20
HadGEM3-GC31-LL	0.133/ 25	5.474/ 23	7.060/ 18	0.082/ 21	21
FGOALS-g3	0.043/ 30	4.692/ 15	6.597/ 15	0.021/ 27	22
HadGEM3-GC31-MM	0.046/ 29	5.473/ 22	6.830/ 17	0.034/ 24	23
CMCC-ESM2	0.149/ 24	9.483/ 27	11.818/ 28	1.778/ 19	24
CESM2-FV2	0.644/ 1	22.634/ 32	25.780/ 32	3.266/ 33	25
UKESM1-0-LI	-0.462/ 34	8.485/ 26	10.298/ 26	1.571/ 14	26
KIOST-ESM	-0.104/ 31	5.081/ 19	7.627/ 25	1.978/ 26	27
CMCC-CM2-SR5	0.288/ 20	11.001/ 28	13.525/ 29	2.065/ 28	28
NorESM2-LM	0.525/ 10	23.957/ 33	26.065/ 33	2.595/ 30	29
NorESM2-MM	0.543/ 8	24.742/ 34	27.579/ 35	3.092/ 31	30
MRI-ESM2-0	0.457/ 14	13.356/ 29	20.047/ 31	3.987/ 34	31
CESM2	0.512/ 11	20.645/ 31	26.216/ 34	4.610/ 35	32
GISS-E2-1-G	-0.518/ 35	5.316/ 35	7.098/ 22	0.063/ 22	33
GFDL-ESM4	-0.153/ 33	7.096/ 25	10.895/ 27	2.210/ 29	34
TaiESM1	0.178/ 23	14.526/ 30	19.292/ 30	3.131/ 32	35

Figure S6. Spatial distributions of the simulated LAI linear trend during the growing season. The number in parentheses in Figure S6 showed the pattern correlation value between the simulations and observations.
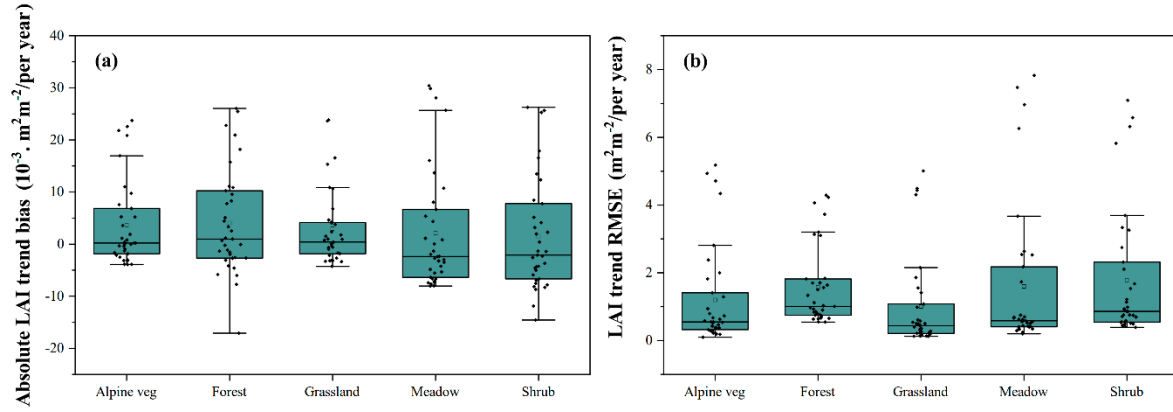
Figure S7. The distribution of bias and RMSE between the simulated and observed LAI trend with 35 CMIP6 models for different vegetation types; the LAI trend is the linear regression trend of the average LAI during the growing season from 1981 to 2014.
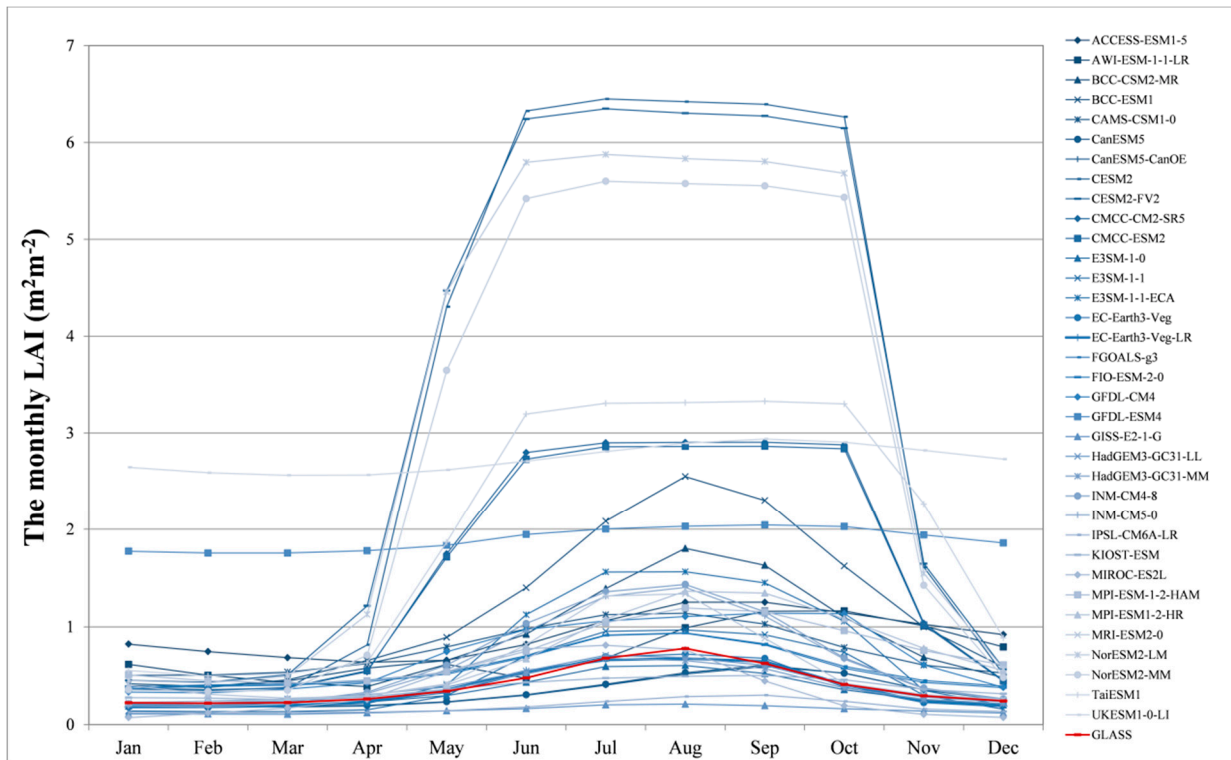

Figure S8. The monthly LAI of 35 CMIP6 models from 1981 to 2014.